A framework to design interaction control of aerial slung load systems: transfer from existing flight control of under-actuated aerial vehicles

Yushu Yu[a], Kaidi Wang[a], Rong Guo[a], Vincenzo Lippiello[b] and Xiaojian Yi[a]

[a]School of Mechatronical Engineering, Beijing Institute of Technology, Beijing 100081, China; [b]Department of Electrical Engineering and Information Technology, University of Naples Federico II, 80125 Naples, Italy

ARTICLE HISTORY
Compiled April 26, 2021

ABSTRACT
This paper establishes a framework within which interaction control is designed for the aerial slung load system composed of an underactuated aerial vehicle, a cable and a load. Instead of developing a new control law for the system, we propose the interaction control scheme by the controllers for under-actuated aerial systems. By selecting the deferentially flat output as the configuration, the equations of motion of the two systems are described in an identical form. The flight control task of the under-actuated aerial vehicle is thus converted into the control of the aerial slung load system. With the help of an admittance filter, the compliant trajectory is generated for the load subject to external interaction force. Moreover, the convergence of the whole system is proved by using the boundedness of the tracking error of vehicle attitude tracking as well as the estimation error of external force. Based on the developed theoretical results, an example is provided to illustrate the design algorithm of interaction controller for the aerial slung load via an existing flight controller directly. The correctness and applicability of the obtained results are demonstrated via the illustrative numerical example.

KEYWORDS
Aerial slung load system, interaction control, under-actuated aerial vehicle, differential flatness

1. Introduction

1.1. Motivation and Background

Aerial slung load transportation has attracted considerable research interests in recent years. An aerial slung load system is usually composed of an under-actuated aerial vehicle, the cable and the load, among which the aerial vehicle provides thrust that is further transferred to the load via the cable. As such, the 3D position of the load can be controlled simultaneously in the aerial slung load system. The aerial slung load system could advance the maneuverability of transportation and also enhance the functions of aerial vehicles, and therefore has found wide applications. As the cable has a light weight, the aerial slung load transportation is more efficient compared to other aerial

CONTACT Xiaojian Yi. Email: yixiaojianbit@sina.cn
This work was supported by the National Natural Science Foundation of China [51505014], Horizon 2020 projects AERIAL-CORE (G.A. 871479) and HYFLIERS (G.A. 779411), and Beijing Institute of Technology Research Fund Program for Young Scholars.

manipulation based on manipulators [1].

Because of the load mass, the aerial slung load system is vulnerable to the swing problem. In order to overcome this problem, many researchers have investigated the motion control problem of slung load system and quite a few results have been reported in the literature. For instance, Lee et al. has examined the dynamics of the aerial slung load system, and designed a geometric controller for the system in [2]. Fang et al. has proposed an energy-based control algorithm in [3] for aerial slung load system. In [4], Romero et al. has developed a controller for the slung load system via energy shaping. By using the backstepping scheme, Silvestre et al. has solved the control problem in [5,6] for the quadrotor slung load system. Leang et al. has exploited the image-based control approach of the aerial slung load system in [7], where the provided algorithm can be used for package delivery. Some other researchers have adopted the planning-based methodology to deal with the swing problem induced by the slung load, see, e.g. [8]. Shan has studied the development of a novel quadrotor load transportation system in [9], which carries payload with four cables. In [10], Kim et al. has proposed the obstacle avoidance algorithm for the aerial slung load system. The data-driven control methodology for the aerial slung load system has also been explored in the literature [11]. According to the aforementioned literature, with the purpose of stabilizing of the load, the controller for the slung load system should be different from that of the under-actuated vehicle motion itself.

Aside from the single aircraft-based slung load system, there have been various research fruits regarding the collaborative load transportation via multiple aerial vehicles. For example, in [12], Lee et al. has proved that by appropriately designing the configuration of the multiple aerial vehicles, the 6D position and attitude of the load can be controlled independently. According to this principle, the motion control of the load transportation using multiple aerial vehicles has been investigated by a number of researchers, see, e.g. [13–17]. Note that the approaches proposed in the above literature have also implemented controllers that are different from the flight controller of aerial vehicles. However, it should be noted that the flight controllers for the under-actuated aerial vehicles are mature enough now [18]. Consequently, it is natural to propose the algorithm which transfers the existing flight controller to the controller of aerial slung load system with a slight modification but at a smaller cost. However, as mentioned earlier, the dynamics and control of the two kinds of system are different. The dynamics of the aerial slung load has higher order than that of under-actuated aerial vehicles. This brings challenge in transferring the flight controller to the aerial slung load system.

It is now recognized that an under-actuated aerial vehicle can be expressed by a differentially flat system with flat output of position and yaw angle [19]. On the other hand, it is known that the aerial slung load system is also differentially flat [2, 20]. The flat output of the aerial slung load system can then be selected as the position and the yaw angle of the load. The differential flatness of the two kinds of systems implies that there is certain similarity that can be utilized to transfer the controller of under-actuated aerial vehicles to that of aerial slung load systems.

Another interesting and significant problem should be mentioned is the interaction control, which is a fundamental requirement in many practical human-machine-environment interface or collaboration such as the robotic system [21]. Such a problem has special significance for the aerial system subject to uncertain disturbances, and therefore has stirred ever-increasing attention, see, e.g. [22–26] for some recent representative works. For instance, in [24], A. Franchi et al. has investigated the aerial physical interaction control problem via IDA-PBC. Lippiello et al. has studied in [25,26] the

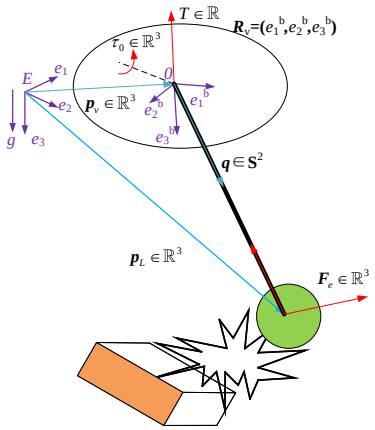

Figure 1.: The aerial slung load physically interacts with the environment, where $e_1 = (1, 0, 0)^T$, $e_2 = (0, 1, 0)^T$, $e_3 = (0, 0, 1)^T$.

interaction control of aerial vehicle via impedance control or passivity-based control. The existing work provides reference for designing the interaction control framework, where it is shown that the interaction controller should enforce the system passive while keeping stable. Note that the impedance control or admittance control is the most popular methodology used in the interaction.

In general, the possible scenarios applying the interaction control for the aerial slung load system include human-in-the-loop control and the collision response. Under the compliant interaction control, the human can manipulate the slung load via physical interaction. In such a case, the human generates external force on the load while the slung load system should react to the force such that it compliantly obeys the commands from the human. Such human-in-the-loop operation is believed to be capable of combining the intelligence of human and the motion accuracy of the machine. On the other hand, when the load collisions with the environment, the interaction control should also let the slung load system react to the collision force compliantly. Fig. 1 indicates a scheme of such scenario.

1.2. Contributions

In this paper, a novel control approach for the aerial slung load system is designed. We consider the external force exerted on the load, which is further utilized for the interaction control design. As only the translational motion of the load is considered in this paper, one aircraft is enough for the control purpose. Therefore, we simply consider the 3D external force on the load. Instead of designing new controller for the interaction control, we aim to directly transfer the exiting aircraft flight controller to the interaction controller of the aerial slung load system. By analyzing the differential flatness of the two kinds of systems, the similarity of the two systems is summarized and adopted in the transfer of the controller. Subsequently, by assuming the boundedness of the attitude tracking error and the force estimation error, the convergence of the whole system is analyzed. We will further apply the theoretical results to derive a detailed interaction controller for the aerial slung system. The key parts of the interaction controller are totally derived from the under-actuated aerial vehicle.

The contributions of the paper can therefore be summarized as follows.

- The similarity of the under-actuated aerial vehicle and the aerial slung load system is analyzed and summarized, which provides a theoretical basis for the controller transfer.
- The theoretical framework is proposed within which the existing flight controller can be conveniently transferred to the interaction control. To the best knowledge of authors, there are no other similar methodologies. The proposed methodology can speed up the development of the interaction controller for the aerial slung load systems.
- The convergence is proved for the overall closed-loop system with uncertainties. From the proof, it is seen that the transfer can be finished from any existing stable flight controller, not for a specific flight controller. The strict proof indicates that the transfer from fight controller to the interaction controller of aerial slung load systems is adequate.

This paper is organized in five sections. In Section 2, the modeling of the two kinds of system and the theoretical basis on the transfer of the controller are derived. The application example by applying the theoretical basis is proposed in Section 3. Numerical examples on a small scale aerial slung load system are presented in Section 4.

2. Modeling and Problem Formulation

2.1. Dynamics of the Aerial Slung Load

In the aerial slung load system, the aircraft and the load are assumed to connect to the cable at the center of the mass (COM). Therefore, the thrust acting on the load only affects the translational motion of the load, while the cable does not affect the rotational motion of the aircraft. The configuration of the cable is expressed in S^2, while the configuration of the under-actuated aerial vehicle is expressed in $SE(3)$.

The configuration space of the entire system is thus $\mathbb{R}^3 \times SO(3) \times S^2 \times \mathbb{R}^3$. We define the coordinate frames as shown in Fig. 1, where frame $\{E\}$ is the inertial frame whose z axis coincides with the gravity direction. The kinematics and dynamics of the aerial slung load system can be expressed as [2],

$$\begin{aligned}
&\dot{p}_L = v_L \\
&(m_V + m_L)(\dot{v}_L - ge_3) = (-q \cdot TR_V e_3 + m_V l(\dot{q} \cdot \dot{q}))q \\
&\dot{q} = \omega_L \times q \\
&\dot{\omega}_L = -\tfrac{1}{m_V l} q \times TR_V e_3 \\
&\dot{R}_V = R_V \hat{\omega}_V \\
&M\dot{\omega}_V + \hat{\omega}_V M\omega_V = \tau
\end{aligned} \tag{1}$$

where $p_L \in \mathbb{R}^3$ and $v_L \in \mathbb{R}^3$ represent the position and velocity of the load expressed in inertial frame; $q \in S^2$ represents the attitude of the cable expressed in inertial frame; $M \in \mathbb{R}^{3\times3}$ is the inertia tensor of the underactuaed aerial vehicle; m_V and m_L are the mass of the vehicle and the load, respectively; g is the acceleration due to gravity; l is the length of the cable; T is the magnitude of thrust provided by the aerial vehicle; $\omega_L \in \mathbb{R}^3$ is the angular velocity of the cable expressed in inertia frame; $R_V \in SO(3)$ is the rotation matrix of the aerial vehicle; $\omega_V \in \mathbb{R}^3$ is the angular velocity of the load and $\tau \in \mathbb{R}^3$ is the torque of the aerial vehicle.

It is observed that the first two elements of (1) define the motion of the load position

of the system, the third and fourth equations define the load attitude of the system, and the last two equations represent the attitude of the aerial vehicle. Assuming that the cable with suspended load is not extending, we have the following constraints for the system

$$q \cdot \omega_L = 0 \tag{2}$$

It can be concluded from (1) that the attitude motion of the aerial vehicle is decoupled from the translational motion and the rotational motion of the load. Therefore, we can further divide system (1) into two parts, namely, the load subsystem described by the first four elements in (1) and the vehicle attitude subsystem expressed by the last two elements in (1).

It is widely recognized that during the physical interaction, there are always forces on the load, and moreover, for the real-world systems, the uncertainties induced by un-modeled dynamics and disturbances are unavoidable. In view of this, by taking into account the external interaction force and uncertainties, the EOM of the load subsystem can be written as follows:

$$\begin{aligned} &\dot{p}_L = v_L \\ &\dot{v}_L = \tfrac{1}{(m_V+m_L)}(-q \cdot TR_V e_3 + m_V l(\dot{q} \cdot \dot{q}))q + ge_3 + \\ &\tfrac{F_e}{m_L} + d_1 \\ &\dot{q} = \omega_L \times q \\ &\dot{\omega}_L = -\tfrac{1}{m_V l} q \times TR_V e_3 + d_2 \end{aligned} \tag{3}$$

where $d_1 \in \mathbb{R}^3$ and $d_2 \in \mathbb{R}^3$, respectively, represent uncertainties due to un-modeled dynamics and external disturbances; $F_e \in \mathbb{R}^3$ is the external force exerted on the load. Here, it is assumed that d_1, d_2, F_e and $\dot{F}_e$ are all bounded. The external interaction force can be generated from humans during the human-in-the-loop operation, or from the contact with the environment.

Problem 1. *Consider the aerial slung load system dynamics (3). Given a desired load position trajectory $p_{L,ref}(t)$ which is smooth enough, consider the tracking error of the aerial vehicle, design the thrust T and the commanded vehicle attitude $R_{V,d}$, such that the actual trajectory $p_L(t)$ compliantly obey the external force F_e, while the tracking error $p_L(t) - p_{L,ref}$ is ultimately bounded.*

2.2. EOM Transformation of the Under-actuated Aerial Vehicle

The dynamics of the slung load system can be obtained from the under-actuated aerial vehicle in terms of the motion of the load. To this end, we first recall the dynamics of the under-actuated aerial vehicle. Moreover, we build the inertial frame whose z-axis coincides with the gravity direction. Then the EOM of the under-actuated aerial vehicle can be expressed as follows:

$$\begin{aligned} &\dot{p} = v \\ &\dot{v} = ge_3 - \tfrac{T}{m} Re_3 + d_4 \\ &\dot{R} = R\hat{\omega} \\ &\dot{\omega} = M^{-1}\left(\tau - \hat{\omega} M \omega\right) + d_5 \end{aligned} \tag{4}$$

where $p \in \mathbb{R}^3$, $v \in \mathbb{R}^3$, $R \in SO(3)$, and $\omega \in \mathbb{R}^3$ are the position, velocity, rotation matrix and angular velocity of the aerial vehicle, respectively; $T \in \mathbb{R}$ and $\tau \in \mathbb{R}^3$ are the thrust and torque of the aerial vehicle, respectively; $d_4 \in \mathbb{R}^3$ and $d_5 \in \mathbb{R}^3$ are the bounded disturbances, respectively.

It is well-known that the under-actuated aerial vehicle is differentially flat with flat output (p, γ), where γ is the yaw angle. It is seen from EOM (4) that the position of the under-actuated aerial vehicle depends on the thrust rather than on the yaw angle. Selecting the flat output variables as the configuration, we can transform the original under-actuated aerial vehicle EOM (4) to the following reduced-order EOM:

$$\begin{aligned} \dot{p} &= v \\ \dot{v} &= ge_3 - \tfrac{T}{m_V} Re_3 + d_4 \\ \dot{r}_3 &= \Omega \times r_3 \\ \dot{\Omega} &= \tau' + d_5' \end{aligned} \tag{5}$$

where $r_3 = R_3 e_3$ is the unit vector along the negative direction of the thrust; $\Omega = -R\hat{e}_3^2\omega$ is the angular velocity projected onto the plane orthogonal to the unit vector Re_3, expressed in the inertial frame; $\tau' = R\omega(-\hat{e}_3)^2\omega + R(-\hat{e}_3)^2\tau$ is the equivalent input and d_5' is the equivalent disturbance.

By defining the reduced-order state as $x_V = (p, v, r_3, \Omega)$, the EOM of the under-actuated aerial vehicle can be written in the following affine format:

$$\dot{x}_V = f(x_V) + h(x_V) \begin{bmatrix} \frac{T}{m_V} \\ \tau' \end{bmatrix} + d_V \tag{6}$$

where $f(\cdot) : \mathbb{R}^9 \times S^1 \mapsto \mathbb{R}^{12}$ and $h(x_V) \in \mathbb{R}^{12\times 4}$ are defined from the EOM (5) and d_V represents the uncertainties.

2.3. EOM Transformation of the Aerial Slung-load System

From the comparison between the EOM of the under-actuated aerial vehicle and the load subsystem of the aerial slung load system (i.e., the first four equations of the slung load system), it can be observed that there are certain similarities. In the slung load system, the cable provides the thrust for the translational motion and the rotational motion perpendicular to the cable.

In the presence of the external interaction force, the actual EOM of the slung-load system can be written as follows:

$$\begin{aligned} \dot{p}_L &= v_L \\ \dot{v}_L &= ge_3 - \tfrac{T_L}{m_L} q + \tfrac{F_e}{m_L} + d_1 \\ \dot{q} &= \omega_L \times q \\ \dot{\omega}_L &= \tau_L + d_2 \end{aligned} \tag{7}$$

where $T_L = \frac{m_L q^T T R_V e_3 + m_L m_V l \|\omega_L\|^2}{m_V + m_L}$ is the cable tension which provides thrust for the load and $\tau_L = -\frac{1}{m_V l}\hat{q} T R_V e_3$ is the projection of the equivalent torque onto the plane orthogonal to q.

Denoting the state $x_L = (p_L, v_L, q, \omega_L)$, the EOM of load subsystem can be written

as follows:

$$\dot{x}_L = f(x_L) + h(x_L) \begin{bmatrix} \frac{T_L}{m_L} \\ \tau_L \end{bmatrix} + d_L + w_e \tag{8}$$

where (T_L, τ_L) is the equivalent input of the load subsystem and $w_e = (0, \frac{F_e}{m_L}, 0, 0)$. We assume the boundedness of d_L as $\|d_L\| \leq b_d$, where b_d is a positive constant.

Comparing the load subsystem EOM (8) with the aerial vehicle reduced EOM (6), we observe that the two EOMs have the same form. However, (8) takes (τ_L, T_L) as the input, which is actually the virtual input. It also can be seen that the relationship between the virtual input (τ_L, T_L) and T, r_3 is expressed by

$$\begin{bmatrix} \frac{T_L}{m_L} \\ \tau_L \end{bmatrix} = A(x_L)Tr_3 + B(x_L) \tag{9}$$

where the matrices $A(x_L) \in \mathbb{R}^{4\times 3}$ and $B(x_L) \in \mathbb{R}^4$ are determined from (7).

Note that the system contains the unknown uncertainties. We start the design of the controller from the nominal EOM. By excluding the uncertainties from (8), the nominal EOM of the load subsystem can be written as follows:

$$\dot{\bar{x}}_L = f(\bar{x}_L) + h(\bar{x}_L) \begin{bmatrix} \frac{T_L}{m_L} \\ \tau_L \end{bmatrix} \tag{10}$$

By the similar line, the nominal EOM of the underactuated aerial vehicle can be written as follows:

$$\dot{\bar{x}}_v = f(\bar{x}_v) + h(\bar{x}_v) \begin{bmatrix} \frac{T}{m_V} \\ \tau' \end{bmatrix} \tag{11}$$

It should be mentioned that for the under-actuated aerial vehicles, there exist various techniques via which the exponential stability of the closed loop system can be guaranteed. Then, without loss of generality, we assume that there exists a controller which stabilizes system (11) exponentially.

The following assumption is also needed for our further development.

Assumption 1. *The attitude tracking controller of the system (4) can render the attitude tracking error bounded, which can be expressed as,*

$$\|R - R_d\| \leq b_1 \tag{12}$$

where $b_1 < 2$ is a small positive constant.

Assumption 1 is rational, The examples of such controller can be found in many kinds of literature, i.e., [18, 27, 28].

2.4. Admittance Filter

In order to realize the compliant interaction control, the following admittance filter is adopted to generate compliant trajectory of the vehicles under external forces,

$$M\ddot{p}_{L,e} + D\dot{p}_{L,e} + Kp_{L,e} = F_e \tag{13}$$

where M, D and K are the desired diagonal mass matrix, damping matrix, and the stiffness matrix, respectively; $p_{L,e} = p_{L,d} - p_{L,ref}$ is the error between the reference trajectory and the compliant desired trajectory. Given the compliant desired trajectory, we then need to design the controller to track the trajectory. Then, the purpose of the controller design is to determine Tr_3 such that $p_L \to p_{L,d}$. However, as there exist unknown uncertainties in the system, $p_L \to p_{L,d}$ is usually difficult to achieve. In this paper, the objective is to make the tracking error $p_L - p_{L,d}$ reside within an allowable region containing origin.

2.5. Transfer from the Controller of Under-actuated Aerial Vehicle

With the purpose of designing and analyzing the interaction control of the slung-load system, let us first review the control of the under-actuated aerial vehicle. From the assumption that there exists a controller which stabilizes system (11) exponentially, and according to the converse theorem of the exponential stability, by defining the tracking error of the nominal system (11) as $\tilde{x}_V$, there is a continuously differentiable function $V : [0 \times \infty] \times D_0 \ni (t, \tilde{x}_V) \to V \in \mathbb{R}$ such that the following inequalities are satisfied:

$$\begin{array}{c} c_1\|\tilde{x}_V\|^2 \leq V \leq c_2\|\tilde{x}_V\|^2 \\ \dot{V} \leq -c_3\|\tilde{x}_V\|^2 \\ \left\| \frac{\partial V}{\partial \tilde{x}_V} \right\| \leq c_4\|\tilde{x}_V\| \end{array} \tag{14}$$

for some positive constants c_1, c_2, c_3 and c_4.

From the similarity between the slung load system and the under-actuated aerial vehicle, the design task of controller for system (5) can be converted to the design of the controller for (8). In this case, for the closed loop nominal load subsystem, there is also the same Lyaponov function $V : [0 \times \infty] \times D_0 \ni (t, \tilde{x}_L) \to V \in \mathbb{R}$ satisfying,

$$\begin{array}{c} c_1\|\tilde{x}_L\|^2 \leq V \leq c_2\|\tilde{x}_L\|^2 \\ \dot{V} \leq -c_3\|\tilde{x}_L\|^2 \\ \left\| \frac{\partial V}{\partial \tilde{x}_L} \right\| \leq c_4\|\tilde{x}_L\| \end{array} \tag{15}$$

We denote the developed virtual control by $\tau_{L,d}, T_{L,d}$. Then the commanded thrust vector for the aerial vehicle can be designed by inverting (9) as follows:

$$T_d r_{3,d} = A^{-1}\left(\begin{bmatrix} T_L \\ \tau_L \end{bmatrix} + h^{-1}(x_L)w_e^* - B \right) \tag{16}$$

where w_e^* is the estimation external force, which can be generated by a stable estimator [29, 30]; A^{-1} and h^{-1} are the pseudo-inverse of A and h, respectively.

Denote the estimation error by $\tilde{w} = w - w^*$. Since the estimator is assumed to be stable, the estimation error is bounded by

$$\|\tilde{w}\| \leq b_2 \tag{17}$$

where b_2 is a positive constant.

Consider the load subsystem (5). Let us denote the state tracking error by $\tilde{x}_L$. Taking into consideration the boundedness of the attitude tracking error and the force estimation error, it can be derived that $\dot{V}$ satisfies

$$\begin{aligned}\dot{V} =& -c_3\|\tilde{x}_L\|^2 + \frac{\partial V}{\partial \tilde{x}_L}\left[A(x_L)(TRe_3 - TR_de_3) + d_L + \tilde{w}\right] \\ \leq& -c_3\|\tilde{x}_L\|^2 + \frac{\partial V}{\partial \tilde{x}_L}\left(\begin{bmatrix} \frac{1}{m_V+m_L}q^T \\ -\frac{1}{m_V l}\hat{q} \end{bmatrix} T(R-R_d)e_3 + \right. \\ & \left. d_L + \tilde{w}\right)\end{aligned} \tag{18}$$

The thrust provided by the aerial vehicle is also bounded, which can be expressed as $\|T\| \leq b_3$, where b_3 is a positive constant. Then we have

$$\begin{aligned}\dot{V} \leq& -c_3\|\tilde{x}_L\|^2 + \left\|\frac{\partial V}{\partial \tilde{x}_L}\right\|\left[\sqrt{\frac{1}{m_V^2+m_L^2} + \frac{1}{m_V^2 l^2}}\right. \\ & \left. b_3 b_1\right] + c_4(b_2+b_d)\|\tilde{x}_L\| \\ \leq& -c_3\|\tilde{x}_L\|^2 + c_4 b_1 b_3\sqrt{\frac{1}{m_V^2+m_L^2} + \frac{1}{m_V^2 l^2}}\|\tilde{x}_L\| + \\ & c_4(b_2+b_d)\|\tilde{x}_L\| \\ \leq& -(1-\theta)c_3\|\tilde{x}_L\|^2 - \theta c_3\|\tilde{x}_L\|^2 + c_5\|\tilde{x}_L\|\end{aligned} \tag{19}$$

where $\theta < 1$ is a positive constant; the positive constant $c_5 = c_4 b_1 b_3\sqrt{\frac{1}{m_V^2+m_l^2} + \frac{1}{m_V^2 l^2}} + c_4(b_2+b_d)$.

Consequently, it can be concluded that the tracking error $\tilde{x}_L$ converges to the region $\{\tilde{x}_L : \|\tilde{x}_L\| \leq \frac{c_2 c_5}{c_1 \theta c_3}\}$ in finite time. The transfer from the flight control of underactuated aerial vehicles to the interaction control of aerial slung load system is therefore achieved.

3. Application Example

3.1. External Force Estimation

Based on the obtained results, we know that there exists a stable estimator for the external force estimation. In this application example, the external force is estimated by using the momentum-based method. We define the momentum of the load as $\rho = m_L v_L$. Then from the EOM of the system we can obtain the derivative of ρ as follows:

$$\dot{\rho} = m_L\dot{v}_L = -T_L q + m_L g e_3 + F_e \tag{20}$$

Next, we define the following estimator for the external force exerted on the load

$$F_e^* = k_I([\rho - \int(-T_L q + m_L g e_3 + F_e^*)dt - \rho(0)]) \tag{21}$$

where $k_I = \text{diag}(k_{I1}, k_{I2}, k_{I3}) \in \mathbb{R}^{3\times3}$ is positive definite diagonal matrix.

3.2. Baseline Controller for Under-actuated Aerial Vehicles

There are various baseline controllers for aerial vehicles. In this paper, we adopt a baseline controller for the under-actuated aerial vehicle from our previous paper [18]. The controller for the under-actuated aerial vehicle is composed of the outer position control loop which outputs the virtual force, and the inner attitude control loop which outputs the torque.

The virtual control force for the translational motion of the aerial vehicles is designed from

$$F_d = m_v(-k_T(\tilde{p}^T, \tilde{v}^T)^T + \ddot{p}_d) \tag{22}$$

where $k_T \in \mathbb{R}^{6\times6}$ is positive definite diagonal matrix; $\tilde{p}$ and $\tilde{v}$ are the position and velocity tracking error, respectively, and p_d is the desired position.

The virtual control input F_d is then mapped to the reference attitude R_d and the thrust T as follows:

$$T = \|mg - F_d\|$$

Then R_d can be solved from the following equation,

$$R_d e_3 = \frac{mg - F_d}{T}$$

The control torque is designed from

$$\tau = -k_\xi \xi_e - k_\omega \omega_e + \hat{\omega} M \omega - M\left(\hat{\omega}\exp(-\hat{\xi}_e)\omega_d - \exp(-\hat{\xi}_e)\dot{\omega}_d\right) \tag{23}$$

where $k_\xi \in \mathbb{R}^{3\times3}$ and $k_\omega \in \mathbb{R}^{3\times3}$ are positive definite diagonal matrices; ξ_e and ω_e are the attitude tracking error and the angular tracking error, respectively.

Projecting the control torque, we can obtain the commanded torque for EOM (5) as follows:

$$\tau' = R\omega(-\hat{e}_3)^2\omega + R(-\hat{e}_3)^2\tau \tag{24}$$

It is seen that by using such a controller, the tracking error of EOM (5) is exponentially stable at origin. Furthermore, from the regular perturbation theorem, the attitude controller can render the attitude tracking error bounded in the presence of d_3.

3.3. Transfer to the Slung Load System

The controller of the under-actuated aerial vehicle can be transferred to control the slung load system. We can write the controller for the aerial vehicle as follows:

$$\begin{bmatrix} \frac{T}{m_V} \\ \tau \end{bmatrix} = C(x_{V,d}, \dot{x}_{V,d}, x_V, K_1) \tag{25}$$

where $x_{V,d}$ is the desired state and $K_1 = (k_T, k_\xi, k_\omega)$ is the parameter set in the vehicle controller.

The controller can therefore be migrated to the load subsystem as follows:

$$\begin{bmatrix} \frac{T_{L,d}}{m_L} \\ \tau_{L,d} \end{bmatrix} = C(x_{L,d}, \dot{x}_{L,d}, x_L, K_2) \tag{26}$$

where $x_{L,d}$ is the desired state of the load subsystem which is generated by the admittance filter, and K_2 is the corresponding parameter set in the load controller.

Subsequently, the virtual control can be mapped to the thrust and attitude of the underactuated aerial vehicle by following (16). The designed attitude thrust is therefore expressed by

$$T_d r_{3,d} = A^{-1}\left(C(x_{L,d}, \dot{x}_{L,d}, x_L, K_2) + h^{-1}(x_L) w_e^* - B\right) \tag{27}$$

3.4. Stability Analysis

The stability analysis is performed by considering the boundedness of the force estimation error, the stability of the original controller for the aerial vehicles, in combination with the results obtained from Section 2.

Theorem 1. *Consider the aerial slung load system (3). The external interaction force is estimated from (21), the desired position of the load is given by the admittance filter (13), and the control law is designed from (22), (24), and (27). Assume the external force is bounded, then the error* $\tilde{x}_L = x_L - x_{L,d}$ *converges to the region* $\{\tilde{x}_L : \|\tilde{x}_L\| \leq \frac{c_2 c_5}{c_1 \theta c_3}\}$ *in finite time, where* $c_5 = c_4 b_1 b_3 \sqrt{\frac{1}{m_V^2 + m_l^2} + \frac{1}{m_V^2 l^2}} + c_4(b_2^* + b_d)$ *with*

$$b_2^* = \frac{1}{m_L}\left(\|F_e\| + \frac{b_4}{\sqrt{k_{I1}^2 + k_{I2}^2 + k_{I3}^2}}\right) \tag{28}$$

Proof. The estimation force error can be estimated from the EOM of the system. Substituting (20) into (21) and taking derivative of F_e^* results in

$$\dot{F}_e^* = k_I(F_e - F_e^*) \tag{29}$$

Defining the estimation error as $\tilde{F}_e = F_e - F_e^*$, then from the external force estimator, we can acquire the estimation error dynamics as follows:

$$\dot{\tilde{F}}_e = -k_I \tilde{F}_e + \dot{F}_e \tag{30}$$

The derivative of the external force is assumed to be bounded, which can be expressed by

$$\|\dot{F}_e\| \leq b_4 \tag{31}$$

Then, the solution of (30) is given by

$$\tilde{F}_e = e^{-k_I t}\tilde{F}_e(0) + \int_0^t e^{-k_I(t-\tau)}\dot{F}_e(\tau)d\tau \tag{32}$$

It is seen from the boundedness of $\dot{F}_e$ that

$$|\tilde{F}_e| \leq |e^{-k_I t}\tilde{F}_e(0)| + b_4 \begin{bmatrix} -\frac{1}{k_{I1}}e^{-k_{I1}t} + \frac{1}{k_{I1}} \\ -\frac{1}{k_{I2}}e^{-k_{I2}t} + \frac{1}{k_{I2}} \\ -\frac{1}{k_{I3}}e^{-k_{I3}t} + \frac{1}{k_{I3}} \end{bmatrix} \tag{33}$$

Then $\tilde{F}_e$ can be further bounded by

$$|\tilde{F}_e(t)| \leq |\tilde{F}_e(0)| + \begin{bmatrix} \frac{b_4}{k_{I1}} \\ \frac{b_4}{k_{I2}} \\ \frac{b_4}{k_{I3}} \end{bmatrix} \leq |F_e(0)| + \begin{bmatrix} \frac{b_4}{k_{I1}} \\ \frac{b_4}{k_{I2}} \\ \frac{b_4}{k_{I3}} \end{bmatrix} \tag{34}$$

which indicates (17). In this case, the constant b_2 in (17) is decided by b_2^* in (28).

From the exponential stability of the closed-loop nominal vehicle system, it can be concluded that under the controller (22), and (24), there exists a Lyapunov function V for the nominal aerial vehicle system satisfying (15). Then following the same steps as (18) - (19), it is seen that the closed-loop aerial slung load system is ultimately bounded, which completes the proof. □

4. Numerical Simulation

In the simulation, a small scale aerial slung load system is considered. The mass of the aerial vehicle is given by $m_V = 2kg$, the mass of the load is $m_L = 1kg$, the length of the cable is $l = 1.2m$, and the inertia tensor of the aerial vehicle is given by $m = \text{diag}(0.025; 0.0636; 0.0809)kg \cdot m^2$.

The external force exerted on the load is shown as the dot-dashed line in Fig. 2. The disturbance expressing the uncertainties is given by

$$d_1 \sim U(-0.5N, 0.5N), d_2 \sim U(-0.5Nm, 0.5Nm) \tag{35}$$

where U represents the uniform distribution.

The interaction controller is transferred from the flight controller using the methodology shown in Section 3. The simulation results are shown in Figs. 3-8. Using the force estimator (21), the estimation result is shown as the solid line in Fig. 2. It is seen that the estimation error of the external force is bounded. The load position tracking is depicted in Fig. 3, which indicates that the actual position tracks the desired position. Under the admittance filter, the desired position reacts to the external force compliantly. The cable attitude expressed in unit vector is illustrated in Fig. 4. It is

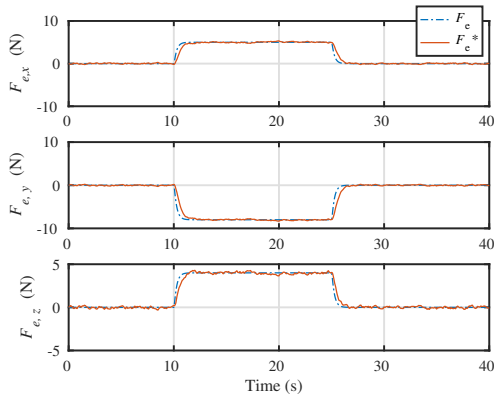

Figure 2.: The actual and the estimated external force acting on the load.

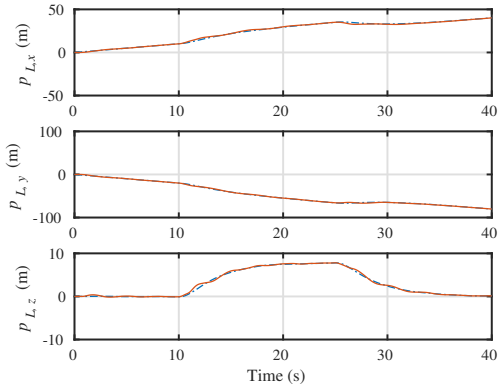

Figure 3.: The desired load position (dot-dashed line) and the actual load position (solid line).

noticeable that the attitude of the cable varies following the external force. Fig. 5 demonstrates the 3D profile of the reference load position, the actual load position, and the position of the aerial vehicle. It is seen that with the proposed interaction control, the desired load position is generated compliantly and tracked by the actual load position. The attitude tracking profile of the aircraft is shown in Fig. 6. The thrust along the cable acting on the load is shown in Fig. 7, while the thrust provided by the under-actuated aircraft is shown in Fig. 8. In summary, all the simulation figures show that the compliant interaction control of the aerial slung load under external force is achieved.

As a comparison, we apply the method presented in [1] here to design the controller for the aerial slung load system. The well-tuned results are shown in Fig. 9 - Fig. 12. It is seen that in the comparison case, the controller cannot handle the interaction force. Therefore, in Fig. 9, the position of the load is not compliant under the external force. Fig. 10 and Fig. 11 present the attitude of the load and the aircraft respectively.

Compared to the baseline controller, it is seen that the performance of our proposed controller is satisfactory. Moreover, our proposed methodology can be used to design the interaction control, therefore can let the system follow the external force compliantly. However, as our proposed controller is transferred from the existing flight controller. The design procedure is much simpler that designing a new controller. The

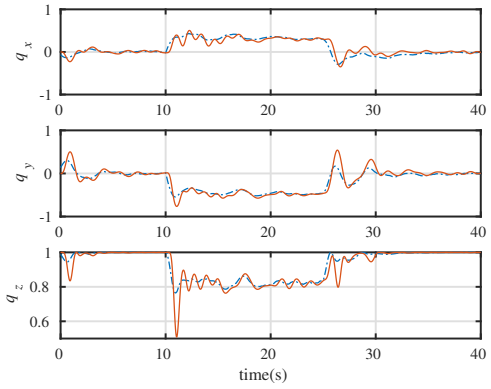

Figure 4.: The commanded load cable attitude (dot-dashed line) and the actual cable attitude (solid line).

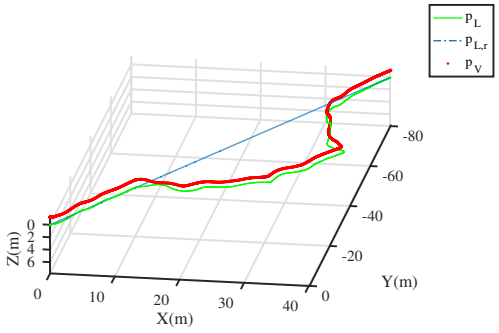

Figure 5.: The 3D profile of the reference load position ($p_{L,r}$), actual load position, and the actual vehicle position.

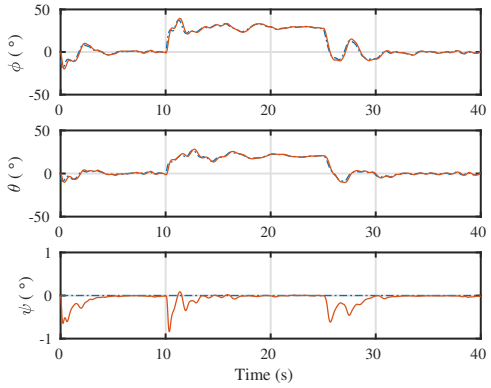

Figure 6.: The aircraft attitude tracking profile, expressed in Euler angles.

comparison provides a reference indicating that we can obtain the interaction controller of the aerial slung load system while ensuring the performance of the controller.

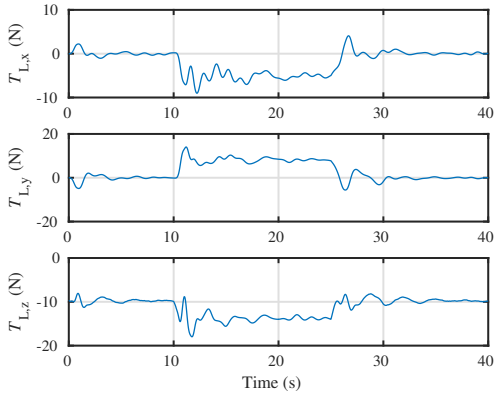

Figure 7.: The thrust vector $T_L q$ provided by the cable.

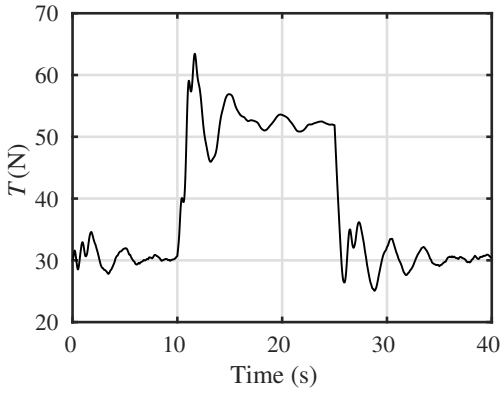

Figure 8.: The thrust magnitude of the aerial vehicle.

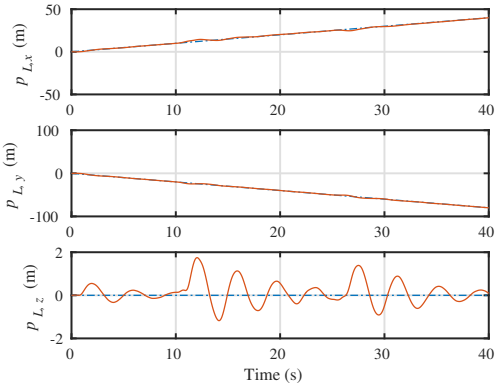

Figure 9.: The desired load position and the actual load position, comparison case.

Remark 1. *In order to apply the proposed methodology into the real world system, we need to design the real world system such that its dynamic equation closes to (1) as much as possible. It is noted that the real world system usually suffers from the problems of latency, either from the sensor or from the actuator. Although it can be proved that the controlled aerial slung load system using the proposed methodology is still stable*

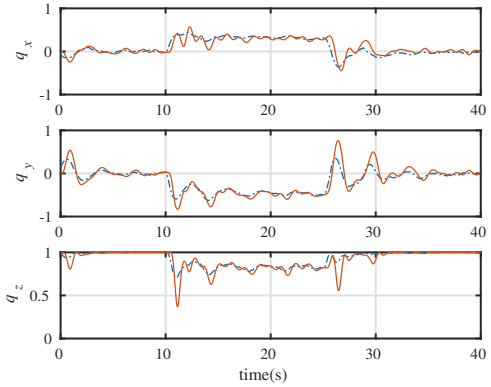

Figure 10.: The attitude of the load, comparison case.

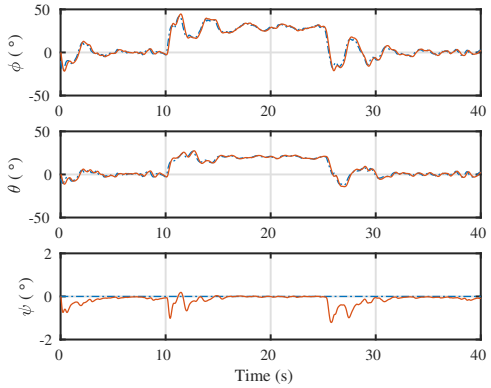

Figure 11.: The aircraft attitude tracking profile, expressed in Euler angles, comparison case.

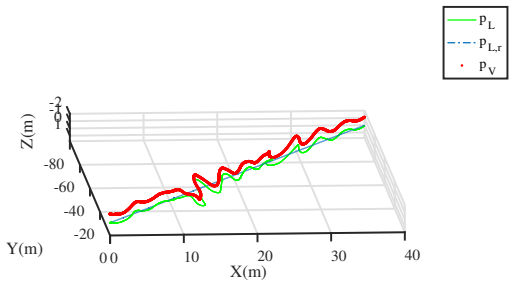

Figure 12.: The 3D profile of the reference load position ($p_{L,r}$), actual load position, and the actual vehicle position, comparison case.

under latency. However, if the latency exceeds certain range, the stability may be hurt. This is also the main possible problem in applying the proposed methodology into the real world system. Applying the proposed methodology into the real world system is also

in our future interests.

5. Conclusions

A methodology has been proposed in this paper on transferring the flight control of under-actuated aerial vehicles to the interaction control of aerial slung load systems. The conversion begins from the comparison of the two kinds of system. By utilizing the differential flatness of the two kinds of system, parts of the EOM of aircraft and the loads have been written in the same form, which has given us the inspiration on how to migrate the control. The uncertainties of the aerial system and the attitude tracking error of the aircraft have been also analyzed. The migration methodology has been proved to be feasible from a series of proof which shows the convergence of the interaction controlled system with uncertainties. The theoretical framework has provided a basis on how to design the interaction control of the aerial slung system. An application example and its numerical simulation from the theoretical framework have been presented in the paper, demonstrating the feasibility of the theoretical framework. Future work can be conducted in several directions. Firstly, the real-world experiments of the proposed work is an interesting topic. Secondly, the proposed work can be extended to the interaction control of slung load transported by multiple aerial vehicles.

References

[1] Y. Yu and X. Ding, "Trajectory linearization control on so(3) with application to aerial manipulation," *Journal of the Franklin Institute*, vol. 355, no. 15, pp. 7072 – 7097, 2018.

[2] K. Sreenath, T. Lee, and V. Kumar, "Geometric control and differential flatness of a quadrotor uav with a cable-suspended load," in *52nd IEEE Conference on Decision and Control*, Dec 2013, pp. 2269–2274.

[3] X. Liang, Y. Fang, N. Sun, and H. Lin, "A novel energy-coupling-based hierarchical control approach for unmanned quadrotor transportation systems," *IEEE/ASME Transactions on Mechatronics*, vol. 24, no. 1, pp. 248–259, Feb 2019.

[4] J. G. Romero and H. Rodriguez-Cortes, "Asymptotic stability for a transformed nonlinear uav model with a suspended load via energy shaping," *European Journal of Control*, vol. 52, pp. 87 – 96, 2020.

[5] D. Cabecinhas, R. Cunha, and C. Silvestre, "A trajectory tracking control law for a quadrotor with slung load," *Automatica*, vol. 106, pp. 384 – 389, 2019.

[6] G. Yu, D. Cabecinhas, R. Cunha, and C. Silvestre, "Nonlinear backstepping control of a quadrotor-slung load system," *IEEE/ASME Transactions on Mechatronics*, vol. 24, no. 5, pp. 2304–2315, Oct 2019.

[7] D. Guo and K. K. Leang, "Image-based estimation, planning, and control of a cable-suspended payload for package delivery," *IEEE Robotics and Automation Letters*, vol. 5, no. 2, pp. 2698–2705, 2020.

[8] B. Xian, S. Wang, and S. Yang, "An online trajectory planning approach for a quadrotor uav with a slung payload," *IEEE Transactions on Industrial Electronics*, vol. 67, no. 8, pp. 6669–6678, Aug 2020.

[9] T. Chen and J. Shan, "A novel cable-suspended quadrotor transportation system: From theory to experiment," *Aerospace Science and Technology*, vol. 104, p.

105974, 2020.
[10] C. Y. Son, H. Seo, D. Jang, and H. J. Kim, "Real-time optimal trajectory generation and control of a multi-rotor with a suspended load for obstacle avoidance," *IEEE Robotics and Automation Letters*, vol. 5, no. 2, pp. 1915–1922, April 2020.
[11] S. Belkhale, R. Li, G. Kahn, R. McAllister, R. Calandra, and S. Levine, "Model-based meta-reinforcement learning for flight with suspended payloads [arxiv]," *arXiv*, pp. 10 pp. –, 2020/04/23.
[12] T. Lee, "Geometric control of quadrotor uavs transporting a cable-suspended rigid body," *IEEE Transactions on Control Systems Technology*, vol. 26, no. 1, pp. 255–264, Jan 2018.
[13] J. Geng and J. W. Langelaan, "Cooperative transport of a slung load using load-leading control," *Journal of Guidance, Control, and Dynamics*, vol. 43, no. 7, pp. 1313–1331, 2020.
[14] D. Sanalitro, H. J. Savino, M. Tognon, J. Cortés, and A. Franchi, "Full-pose manipulation control of a cable-suspended load with multiple uavs under uncertainties," *IEEE Robotics and Automation Letters*, vol. 5, no. 2, pp. 2185–2191, April 2020.
[15] T. Bacelar, J. Madeiras, R. Melicio, C. Cardeira, and P. Oliveira, "On-board implementation and experimental validation of collaborative transportation of loads with multiple uavs," *Aerospace Science and Technology*, vol. 107, p. 106284, 2020.
[16] E. Rossi, M. Tognon, R. Carli, L. Schenato, J. Cortés, and A. Franchi, "Cooperative aerial load transportation via sampled communication," *IEEE Control Systems Letters*, vol. 4, no. 2, pp. 277–282, April 2020.
[17] G. Cardona, D. Tellez-Castro, and E. Mojica-Nava, "Cooperative transportation of a cable-suspended load by multiple quadrotors," vol. 52, no. 20, Chicago, United states, 2019, pp. 145 – 150.
[18] Y. Yu and X. Ding, "A global tracking controller for underactuated aerial vehicles: Design, analysis, and experimental tests on quadrotor," *IEEE/ASME Transactions on Mechatronics*, vol. 21, no. 5, pp. 2499–2511, 2016.
[19] D. Mellinger and V. Kumar, "Minimum snap trajectory generation and control for quadrotors," in *2011 IEEE International Conference on Robotics and Automation*, 2011, pp. 2520–2525.
[20] J. Zeng, P. Kotaru, M. W. Mueller, and K. Sreenath, "Differential flatness based path planning with direct collocation on hybrid modes for a quadrotor with a cable-suspended payload," *IEEE Robotics and Automation Letters*, vol. 5, no. 2, pp. 3074–3081, April 2020.
[21] A. Ajoudani, C. Fang, N. Tsagarakis, and A. Bicchi, "Reduced-complexity representation of the human arm active endpoint stiffness for supervisory control of remote manipulation," *The International Journal of Robotics Research*, vol. 37, no. 1, pp. 155–167, 2018.
[22] A. Albu-Schaffer, C. Ott, U. Frese, and G. Hirzinger, "Cartesian impedance control of redundant robots: recent results with the dlr-light-weight-arms," in *2003 IEEE International Conference on Robotics and Automation (Cat. No.03CH37422)*, vol. 3, 2003, pp. 3704–3709 vol.3.
[23] R. Rashad, F. Califano, and S. Stramigioli, "Port-hamiltonian passivity-based control on se(3) of a fully actuated uav for aerial physical interaction near-hovering," *IEEE Robotics and Automation Letters*, vol. 4, no. 4, pp. 4378–4385, 2019.
[24] B. Yüksel, C. Secchi, H. H. Bülthoff, and A. Franchi, "Aerial physical interaction

via ida-pbc," *The International Journal of Robotics Research*, vol. 38, no. 4, pp. 403–421, 2019.

[25] F. Ruggiero, J. Cacace, H. Sadeghian, and V. Lippiello, "Impedance control of vtol uavs with a momentum-based external generalized forces estimator," in *2014 IEEE International Conference on Robotics and Automation (ICRA)*, 2014, pp. 2093–2099.

[26] F. Ruggiero, J. Cacace, H. Sadeghian, and V. Lippiello, "Passivity-based control of vtol uavs with a momentum-based estimator of external wrench and unmodeled dynamics," *Robotics and Autonomous Systems*, vol. 72, pp. 139 – 151, 2015.

[27] C. G. Mayhew, R. G. Sanfelice, and A. R. Teel, "Quaternion-based hybrid control for robust global attitude tracking," *IEEE Transactions on Automatic Control*, vol. 56, no. 11, pp. 2555–2566, 2011.

[28] T. Lee, "Geometric tracking control of the attitude dynamics of a rigid body on SO(3)," in *Proc. American Control Conference*, San Francisco, CA, 2011, pp. 1200–1205.

[29] Q. Liu and Z. Wang, "Moving-horizon estimation for linear dynamic networks with binary encoding schemes," *IEEE Transactions on Automatic Control*, pp. 1–1, 2020.

[30] Q. Liu, Z. Wang, X. He, and D. Zhou, "Event-based distributed filtering over markovian switching topologies," *IEEE Transactions on Automatic Control*, vol. 64, no. 4, pp. 1595–1602, 2019.